Sussex Research Online

Exploratory studies on azido-bridged complexes (Ni2+ & Mn2+) as dual colourimetric chemosensors for S2- and Ag+: combined experimtal and theoretical outcome with real field application

Article (Accepted Version)

Pandit, Nithun Ranjan, Bej, Sourav, Mondal, Ananya, Ghosh, Meenakshi, Kostakis, George E, Powell, Annie K, Banerjee, Priyabrata and Biswas, Biplab (2020) Exploratory studies on azido-bridged complexes (Ni2+ & Mn2+) as dual colourimetric chemosensors for S2- and Ag+: combined experimtal and theoretical outcome with real field application. Dalton Transactions. ISSN 1477-9226

This version is available from Sussex Research Online: http://sro.sussex.ac.uk/id/eprint/93261/

This document is made available in accordance with publisher policies and may differ from the published version or from the version of record. If you wish to cite this item you are advised to consult the publisher's version. Please see the URL above for details on accessing the published version.

Copyright and reuse:
Sussex Research Online is a digital repository of the research output of the University.

Copyright and all moral rights to the version of the paper presented here belong to the individual author(s) and/or other copyright owners. To the extent reasonable and practicable, the material made available in SRO has been checked for eligibility before being made available.

Copies of full text items generally can be reproduced, displayed or performed and given to third parties in any format or medium for personal research or study, educational, or not-for-profit purposes without prior permission or charge, provided that the authors, title and full bibliographic details are credited, a hyperlink and/or URL is given for the original metadata page and the content is not changed in any way.

http://sro.sussex.ac.uk

Journal Name

ARTICLE

Exploratory studies on azido-bridged complexes (Ni^{2+} & Mn^{2+}) as dual colourimetric chemosensors for S^{2-} and Ag^{+}: combined experimtal and theoretical outcome with real field application

Received 00th January 20xx,
Accepted 00th January 20xx

DOI: 10.1039/x0xx00000x

www.rsc.org/

Nithun Ranjan Pandit,[¥a] Sourav Bej,[¥b,c] Ananya Mondal,[a,d] Meenakshi Ghosh,[d] George E. Kostakis,[e] Annie K. Powell,[f] Priyabrata Banerjee*[b,c] and Biplab Biswas*[a]

We report two isostructural dinuclear transition metal complexes $[M_2(HL)_2(N_3)_4]$, where M = Ni^{2+} (**BS-1**), Mn^{2+} (**BS-2**) and HL is (2-methyl-2-((pyridin-2-ylmethyl)amino)propan-1-ol) and investigate their as molecular sensors towards hazardous entities. **BS-1** shows high selectivity towards the S^{2-} & Ag^{+} ions, observed by ease naked eye colour change, and its detection limit in aqueous solutions for the S^{2-} ion was calculated at 0.55 µM with a binding constant of $3.28x10^5$ M^{-1}, while the limit for the Ag^{+} ion is 21.8 µM. Notably, **BS-2** shows good selectivity towards the Ag^{+} ion with a detection limit of 10.84 µM. Spectroscopic and DFT studies shed lighton the mechanistic course of interaction of host and guest entity, suggesting a sulphide mediated reduction of azide mechanism. In a nutshell, these simple transition metal complexes were exploited for discriminately detect hazardous analytes with a real field application in analytical science (*via.* "**Dip-Stick**" approach) as well as engineering science which keeps a footprint in recent advancement of supramolecular chemistry.

Introduction

Azides play a ubiquitous role in coordination chemistry and specific the inorganic azide, N_3^-, represents the most widely used form to date. The coordination modes of N_3^-vary from monodentate to hexadentate (*vide.* **Scheme S1**) with the tetra- & hexa-dentate modes representing the more rare examples,[1] and notably several complexes of high nuclearity and coordination polymers are reported.[2,3] The distinct structural features of azido-based compounds depend mainly on the nature of the coordinated co-ligands and to some extent on the nature of the central metal ion (M^{n+}); its oxidation state, the coordination number and geometry of the complex; thus, the lack of synthetic control represents a significant disadvantage in the synthesis of the azido complexes. The targeted syntheses of azido-bridged complexes with a particular number of metal centres and binding mode of the azide (co-)ligands as well the conversion of a mononuclear metal-azido complex into an heterodinuclear azido-bridged are challenging tasks.[3] Apart from the fundamental interest in the coordination chemistry of this ion with metal complexes, azido bridged complexes exhibit interesting magnetic properties as well can be used to transfer an "N" atom to a substrate;[4] thus their application as sensing probes towards external toxic analytes is an underdeveloped research area.[5]

H_2S is a highly toxic and flammable gas and, like carbon monoxide and nitric oxide, represents one of the most recognised gasotransmitters.[6] In terms of toxicity, its impact is comparable to that of cyanide intoxication in the human body. H_2S is indeed an essential endogenous gaseous signalling molecule for controlling the cardiovascular, endocrine, neuronal, etc.[7,8] The limit of H_2S in human blood is in the range of 10-100 µM and the central nervous system is in the range of 50-160 µM. A higher level of H_2S imposes harmful effects such as cytotoxicity and irritation to the skin and mucosa of the living bodies.[9] Long exposure of high concentrations of H_2S to the human body results in severe damage to the eyes, respiratory system and nervous system, and it may even lead to a fatal consequence.[10,11] This toxic analyte is present mainly in rivers and/or flowing waters as HS^-, originating from the activity of the sulfate-reducing bacteria and the disintegration of many organic compounds. Also, H_2S can pollute the adjacent environment during many industrial activities, including petrochemical treatment and paper as well as leather manufacturingindustries.[12] Due to its lethal toxicity, H_2S possesses a significant pollution index.Consequently, the detection of this lethal analyte is of immense importance, in

[a] Department of Chemistry, Presidency University, 86/1, College Street, Kolkata 700073, India biplab.chem@presiuniv.ac.in http://presiuniv.ac.in/web/; Tel: +919734246721
[b] .Surface Engineering & Tribology Group, CSIR-Central Mechanical Engineering Research Institute, Mahatma Gandhi Avenue, Durgapur 713209, India, pr_banerjee@cmeri.res.in,priyabratabanerjee16@gmail.com; Web: www.cmeri.res.in,www.priyabratabanerjee.in; Tel: +91 343 6452220, +91 9433814081
[c] Academy of Scientific & Innovative Research (AcSIR), AcSIR Headquarters CSIR-HRDC Campus, Postal Staff College Area, Sector 19, Kamla Nehru Nagar, Ghaziabad – 201002, Uttar Pradesh, India
[d] Vidyasagar College for Women, 39 Sankar Ghosh Lane, Kolkata, 6, West Bengal, India
[e] School of Life Sciences, University of Sussex, Falmer, BN19QG, United Kingdom
[f] InstitutfürAnorganischeChemie, Karlsruhe Institute of Technology (KIT), Engesserstr. 15, D-76131 Karlsruhe, Germany.
Electronic Supplementary Information (ESI) available: [Crystal, IR, UV-Vis, MS and DFTData]. See DOI: 10.1039/x0xx00000x
¥Equal Contribution

order to keep our environment clean, healthy and safe. Currently, many analytical methods are available for H_2S measurement including gas chromatography, electrochemical, electrogenerated chemiluminescence and inductively coupled plasma-atomic emission spectrometry methods. However, these methods require sophisticated instrumentation and are not suitable for rapid on-field analysis. Recently, a microplate reader assay was reported for determination of sulphides;[13] however, this method uses UV measurement technique at the mid UV region (200-300 nm) which could suffer from several interferences, and it is not selective for H_2S, besides, the used reaction was relatively slow that needs a couple of minutes to complete the detection procedure. The colourimetric based analysis is rather simple, rapid and confers high sensitivity. Chromogenic reagents that use the reducing ability sulphide or nucleophilicity, in addition to reagents based on sulfide ability as a ligand to exchange with metal complexes have been reported. However, many of these methods incorporate environmentally harmful organic solvents or toxic metals, require complicated or expensive synthetic procedures for the sensing probes and suffer from the slowness of their reactions with H_2S.

Silver (Ag^+) is a toxic cationic contaminant and displays fundamental roles concerning human health and the environment. This analyte is widely used in various industrial processes such as photography imaging, soldering production, electrical and electronics, automobiles and as a catalyst in oxidation reactions.[14] However, improper disposing of this metal may damage aquatic lives and may accumulate in the human body through the food chain. Prolonged accumulation of this heavy metal in the human body, may displace essential elements like Ca^{2+} & Zn^{2+} ions in hydroxylapatite in the bone. Moreover, exposure of these silver ions through binding with various metabolites such as amine, carboxyl groups *etc.* and inactivating sulfhydryl enzymes have also been discovered. The high concentration of Ag^+ can affect human health profusely by damaging the brain, nerve and immune system. Therefore, analysis of this deadly analyte from food resources is of great importance. Some of the traditional methods such as spectrophotometry, atomic absorption spectrometry, voltammetry, potentiometry and inductively coupled plasma atomic emission spectrometry have been used for the detection of silver ions. However, these methods have many drawbacks, including labour-intensive, high cost and tedious sample preparation methodology. Thus the development of sensors with high selectivity and sensitivity to detect Ag^+ in environmental and food samples is a timely topic of high interest.

A recent literature survey reveals that most of the sensors focus on detecting a single particular analyte. The selective detection of more than one analytesby a single molecular entity from the aqueous or semi-aqueous medium is a challenging task because of their different solvation energy, charge density, kinetic diameter *etc.* Bearing all these in mind, we envisaged that azido based low nuclearity complexes might be suitable candidates to serve this purpose. We report herein the synthesis and characterisation (SCXRD, UV-Vis, FT-IR,ESI-MS, TGA) of two azido bridged dinuclear complexes $[M_2(HL)_2(N_3)_4]$, where M = Ni^{2+} (**BS-1**), Mn^{2+} (**BS-2**) and HL is (2-methyl-2-((pyridin-2-ylmethyl)amino)propan-1-ol) and their use as dual sensors for selective detecting of S^{2-} and Ag^+. Theoretical studies shed light on the detection ability of these molecular sensors implementing that, for the S^{2-}analyte a sulphide mediated reduction of the azide centresoccurs.[15] **BS-1** was also incorporated towards the fabrication of "paper-strips" to develop an instantaneous detection of S^{2-}/H_2S by "Deep-stick" method without the help of any costly instrumentation.

Experimental Section

The preparatory chemicals (reagents, solvents) were of analytical grade and commercially available in the market and were used as received without any further purification. Anions of tetrabutylammonium fluoride, chloride, cyanide, nitrate, acetate and perchlorate were purchased from Sigma Aldrich Pvt.Ltd. Tetrabutylammonium bromide, iodide, the sodium salt of sulphide and hydrogen sulphate were purchased from Alfa Aesar company. The required solvents, like DMSO, methanol, acetonitrile, DMF and water were purchased in spectroscopic grade from Merck (India) Pvt. Ltd and were used without any further purification.

Synthesis of $[Ni_2(HL)_2(N_3)_4]$ (BS-1). To 25 ml methanol 0.112 g (1 mmol) pyridine-2-aldehyde and 0.089 g (1 mmol) 2-amino-2 methyl-1-propanol were stirred for half an hour in room temperature. The colour of the mixture turned colourless to light yellow. One equivalent of $Ni(OAc)2.4H_2O$, 0.249 g (1 mmol) was added to the reaction mixture, and the colour changed from yellow to green instantly. After 30 minutes, 0.130 g (2 mmol) NaN_3 was added to it in order to bring the metal centres in close proximity. The reaction mixture was stirred overnight, and it was filtered and kept for slow evaporation. Yellowish orange coloured X-ray quality crystals were obtained on slow evaporation of 9:1 mixture of Methanol-DMF solution. Elemental analysis calculated for the dried sample $C_{26}H_{42}N_{18}Ni_2O_4$ resulted; found (%): C: 39.49, H: 4.96, N: 31.35; whereas cald. (%): C:39.62; H:5.37; N: 31.99 IR (KBr, cm^{-1}): 2981, 2056, 1586, 1440, 1353.

Synthesis of $[Mn_2(HL)_2(N_3)_4]$ (BS-2). To 25 ml of methanol 0.112 g (1 mmol) Pyridine-2-aldehyde and 0.089 g (1 mmol) 2-amino-2 methyl-1-propanol were stirred magnetically for half an hour. The colour of the mixture turned colourless to light yellow. One equivalent of $Mn(OAc)2.4H_2O$, 0.245g (1 mmol) was added to the reaction mixture, and the colour changed to dark brown instantly. After 30 minutes, 0.130 g (2 mmol) NaN_3 was added to it, and the colour of the reaction mixture changed to yellowish-brown. The reaction mixture was stirred overnight, and it was filtered and kept for slow evaporation. Greyish dark solid compound was collected after a few days. X-ray quality crystals were obtained on slow evaporation of MeCN solution. Elemental analysis was calculated for the dried sample $C_{20}H_{28}N_{16}Mn_2O_2$ resulted; found (%): C: 37.77, H: 4.43, N: 35.71; whereas cald. (%): C:37.86; H: 4.45; N: 35.32.IR (KBr, cm^{-1}):2068, 1604, 1589, 1398. ESI-MS (m/z): 611.19 [$M-N_3+H_2O]^+$.

Preparation of stock solutions of anions & cations. One millimole inorganic salts of the respective anions were dissolved in distilled water to get 10^{-1}mol/L aqueous solution. The stock solutions were then diluted to the desired concentration. Likewise, the cationic solutions were prepared by dissolving the 1 millimole cationic salts in $MeCN/H_2O$ (9:1, *v/v* pH ~ 7.4).

Apparatus. The UV-Visspectra were recorded in a CARY60 spectrophotometer. ESI-MS mass spectra were done on an Advion make compact mass spectrometer (serial no. 3013-0140). The infrared spectra were recorded using a PerkinElmer make FT-IR Spectrum 100 spectrophotometer. Thermo gravimetric analysis has been carried out using NETZSCH STA 449F1 Jupiter instrument Perkin Elmer Pyris™ 1 TGA analyser in the temperature range of 40–1000 ^{0}C at the heating rate of 10.0 °C/min under N_2 atmosphere with the flow rate of 20.0 mL/min. Crystallographic data for **BS-1** and **BS-2** were collected at the Institute of Nanotechnology, Karlsruhe Institute of Technology. The crystals were kept at a steady T = 298(2) and 180(2) K during data collection, respectively. All

This journal is © The Royal Society of Chemistry 20xx

crystal structures were then refined on Fo^2 by full-matrix least-squares refinements using SHELXL.[16] Geometric/crystallographic calculations were performed using Olex2package,[17] and graphics were prepared with Crystal Maker.[18] Structures BS-1 and BS-2 have been given CCDC deposition numbers 1981492-1981493, respectively.

Results and discussion

BS-1 and **BS-2** are isostructural and crystallise in P 2_1/c and P2_1/n space groups, respectively. Both compounds consist of a discrete neutral dinuclear unit, and only the structure of BS-1 will be described. Selected bond lengths and bond angles are given in **Tables S1 & S2**. The dimer is linked via the two bridging nitrogen atoms (N6) of the azide anions by end on (1,1) fashion[19]. Each metal centre is in a distorted octahedral NiN_5O environment by a similar kind of ligand moiety (Schiff base) formed in-situ by the condensation of pyridine-2-aldehyde and 2-amino-2 methyl-1-propanol. Each coordination sphere of the metal ion is occupied by the pyridyl nitrogen (N1), imino nitrogen (N2) and oxygen (O1) of the Schiff base along with the two bridging nitrogen atoms (N6) coming from azide anions and nitrogen atom (N3) of the terminal azide anion which is directly attached with each of the metal centres. The oxygen O(1) atom of the Schiff base is protonated even after the complex formationand may participate in hydrogen bonding interactions with the solvent. Two azide ions bridged between two Ni centres and another two azide ions which are directly attached (terminal azide) with each of the Ni balances the +2 oxidation state of each Ni centres. All the bond distances in the basal planes fall in the range 2.021-2.107Å. The complex is centrosymmetric in which azides bridge the metal centres with the centre of the symmetry at the centre of the Ni_2N_2 parallelogram core. Ni(II) centres bridged through azide ions are separated by a comparatively long distance at Ni(1)-N(6)-Ni(1) 3.243 Å. Two Ni centres including the bridged azide ions are almost planar and the Ni-N-Ni bond angles are 102.4(1)°. Azide ions which are directly attached with the each Ni centres are almost planar to the basal plane containing two Ni centres and this is depicted from the bond angle Ni(1)-N(3)-N(4) (120.6(2)°). Two hexa-coordinated Ni centres have slight distortion from the perfectly octahedral geometry which can be depicted from the N(6)-Ni(1)-N(3) bond angle which is 167.1(1)°.

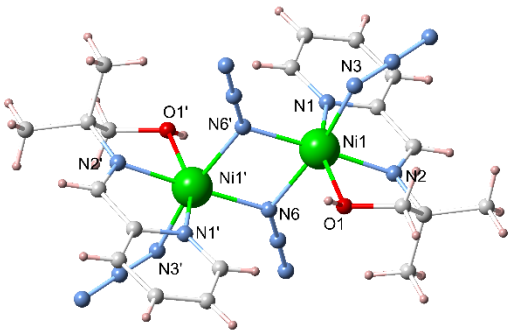

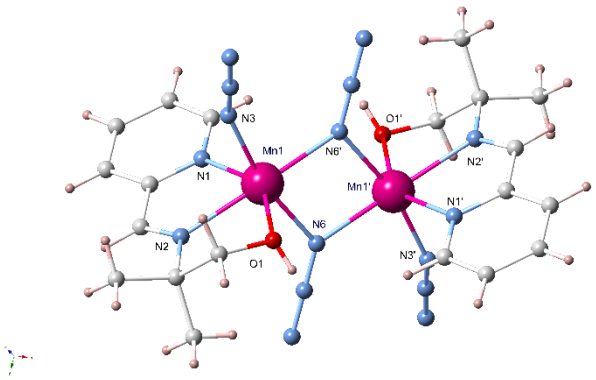

Fig. 1 The dinuclear complexes **BS-1**(up) and **BS-2** (down).

Colourimetric responses of BS-1 towards S^{2-} in an aqueous medium. The colourimetric response of the **BS-1**(10^{-5} M) in DMSO medium towards different anions was examined, and found that a drastic colour change from light yellow to brown was observed only for sulphide (**Fig. 2 up**) whereas for other anions the colour remained unaltered.

Visual Colorimetric responses of BS-1 with Ag^+ and other cations. The colourimetric responses of BS-1 towards different cations in semi-aqueous ($MeCN/H_2O$; *v/v* 9:1) medium has been investigated. Decolourisation was observed only in the presence of Ag^+ (**Fig. 2 down**). The chemoreceptor remained silent in the presence of other cations which described its selectivity towards the heavy metal Ag^+ only.

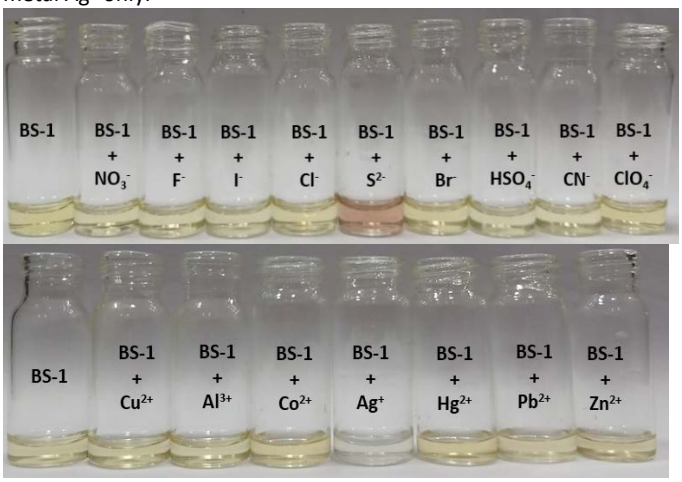

Fig. 2 (up) Visual effects of **BS-1** in DMSO medium towards different anions in purely aqueous phase (down) Visual effects of **BS-1** in DMSO medium towards different cations in semi-aqueous ($MeCN/H_2O$, *v/v* 9:1) phase.

Spectro-photometric properties of the chemoreceptor BS-1 with Ag^+ and S^{2-}. UV-Vis titration of BS-1. In order to investigate the interaction of the BS-1 with various anions & cations, UV-Vis titration of the chemosensor was carried out at room temperature using the salt solution of the targeted analytes. The spectrum of **BS-1** in DMSO medium exhibited a discrete peak at 275 nm due to the ligand-localised π-π* transition. The π-π* transition corresponds to the transition in the aromatic pyridinemoiety.[20] In addition to this, a minor contribution from low-energy transition is assigned due to ICT (Intra-ligand change transfer)overlapped with a MLCT ($M_{d\pi}$-HL_{π^*}) leading to the overall colouration of the metal complex.[21] The addition of $S^{2-}$to the chemosensor solution leads to the change of electronic property *via* reduction of N_3 to NH_2 of **BS-1**. The peak at

275 nm was reduced with the concomitant increment of the MLCT peak at 315 nm (**Fig. 3**) with a well-anchored isosbestic point at 290 nm. This leads to a vivid naked eye colour change from light yellow to brown.

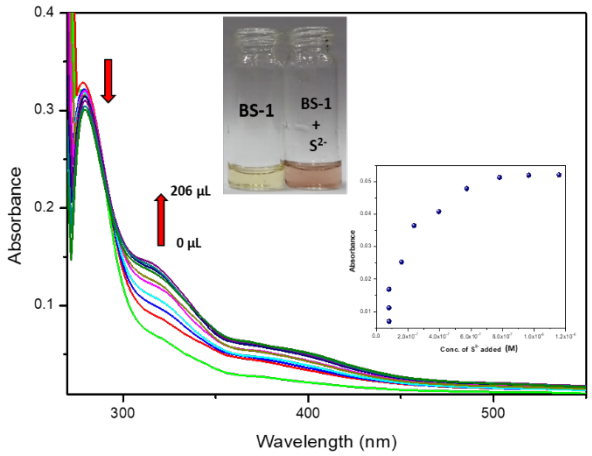

Fig. 3 UV-Vis absorbance change of **BS-1** (10^{-5} M) in DMSO medium with the gradual addition of S^{2-}(10^{-4} M) in an aqueous medium at room temperature. Inset: absorbance at 315 nm as a function of the equivalence of S^{2-} ions added.

The colour change indicates an intermolecular reduction of the coordinated azides. The enhancement of thepeak at the 315 nm and presence of isosbestic point further affirmed a host: guest complexation (herein **BS-1** as host & S^{2-} as a guest). The binding constant calculated from B-H plot was found to be 3.28×10^5 M^{-1} (**Fig. S4**). A good linear functionof absorbance at 315 nm *vs.* S^{2-} concentration was observed in the concentration range of 0-0.2 µM. The LOD was found to be 0.55 µM. (**Fig. S5**).

When organo-aqueous solution of Ag^+ was added to the chemoreceptor **BS-1** solution, the response of **BS-1** was utterly different from that of the anionic responses. The peak at 275 nm was diminished slightly with the concomitant generation of a new peak at 410 nm (**Fig. 4**). In this plot, no further increment of the absorbance intensity upon further addition of 510 µL of Ag^+ ions indicated the saturation of the absorbance intensity of the sensory receptor. The generation of the new peak followed by gradual increment occurred due to the formation of [BS-1-Ag^+] ion complex. According to Pearson's theory, "Soft" metal ions, such as Ag^+ ions, prefers "soft donors" centres for plausible complexation. In designing the chemosensor for Ag^+ ions, soft donor centres like sulphur or nitrogen should be present in the sensing chemosensor molecule. Therefore, the electron-rich azide sub-units present in the **BS-1** may provide good binding sites for Ag^+ ion [22,23]. As an artefact, the colour of the chemosensor **BS-1** changes from light yellow to colourless due to changes in electronic property. The generation of the new peak at 410 nm followed by the formation of the isosbestic point at 300 nm affirmed the interaction between host and guest analyte, which drove the spectra towards the red-shifted region. The binding constant calculated from B-H plot was found to be 0.55×10^3 M^{-1}. A good linear-absorbance response at 410 nm as a function of Ag+ concentration (0-0.81 µM) was obtained. Its regression equation was $A\text{-}A_0 = -5.28 \times 10^{-5} + 1.59 \times 10^4 \times [Ag^+]$. The detection limit was calculated using 3σ/k method and was found to be 21.8 µM (**Fig. S6**, **Fig. S7**).

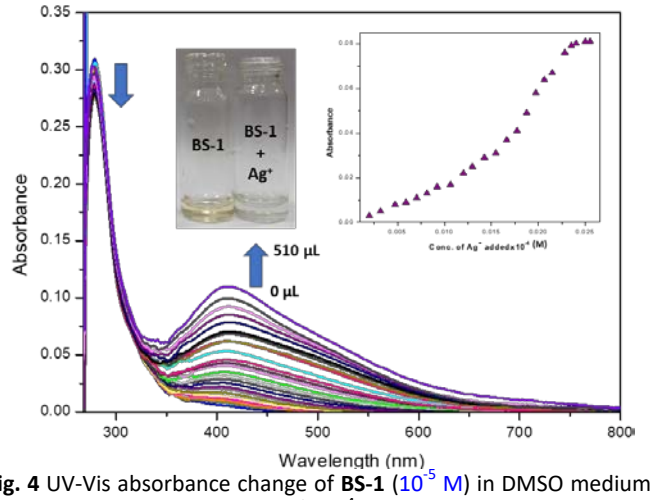

Fig. 4 UV-Vis absorbance change of **BS-1** (10^{-5} M) in DMSO medium with the gradual addition of Ag^+(10^{-4} M) in MeCN/H_2O medium at room temperature. Inset: absorbance at 410 nm as a function of the equivalence of Ag^+ ions added.

The selectivity of BS-1 towards other competitive anions and cations in aqueous and organo-aqueousmedium respectively. In order to appraise the selectivity of our developed chemosensor, we have investigated the effect of other anions & cations on the response of **BS-1** (**Fig. S8**) clearly illustrates that the sensor molecule is not responsive towards other competitive anions like F^-, Cl^-, Br^-*etc.* in a similar environment. Similarly, this probe was only selectively responsive towards Ag^+ even in the co-existence of other cations (**Fig. S9**) showing the unambiguous selectivity of the **BS-1** towards Ag^+ in solution.

Effect of pH on the sensing phenomenon. To check the stability of the sensing mechanism in a more harsh environment, we have studied the effect of pH starting from pH 3-9 using HEPES buffer (**Fig. S10**). It was observed that in extreme acidic condition (e.g; pH 3,4), there were slight visual or spectroscopic changes of the chemoreceptor **BS-1** towards the detection of S^{2-}, which may be due to the protonation of the S^{2-}/HS^- centre. As a result, S^{2-} converted into H_2S gas and concomitant amount of $S^{2-}$was getting reduced from the solution. Likewise in basic condition, the S^{2-} probably reacted with the cation like Na^+ (from NaOH), and formation of solid Na_2S took place due to common ion effect. Hence, the sensor molecule **BS-1** was unable to detect the targeted analyte (S^{2-}) from the aqueous phase in extreme basic condition. In this context, the sensor molecule can be successfully applied in the physiological pH range (5-7).

Colorimetric responses of BS-2 towards Ag^+ in the semi-aqueous medium. The colourimetric responses of **BS-2** (10^{-4} M, DMSO) with different cationic solutions in MeCN:H_2O (9:1; *v/v*) medium was investigated. The colour of the sensor solution was changed (from greyish-yellow to decolouration) drastically (**Fig. 5**) upon addition of Ag^+ whereas other cationic contaminants like Cu^{2+}, Co^{2+}, Zn^{2+}, Pb^{2+} *etc.* remained silent upon interaction with the sensor molecule **BS-2**.

This journal is © The Royal Society of Chemistry 20xx

Fig. 5 Visual effects of BS-2 (10^{-4} M, DMSO) towards differentcations in organo-aqueous (9:1; v/v) phase

Spectrophotometric properties of the chemoreceptor BS-2 with Ag^+. UV-Vis spectra of BS-2 (10^{-4} M) in DMSO was performed which showed intense band centred at 270 nm. This low-energy band was assigned as π-π* transition of the aromatic moiety of the ligand HL. Interestingly, the colour of the **BS-2** was decoloured from greyish yellow to faint yellow (**Fig. 6**) upon interaction with the targeted analyte, Ag^+ ion. The gradual diminish in the absorption peak position infers change in the electronic property within the molecular scaffold upon gradual addition of Ag^+. Herein, the electron rich azide centres provide an excellent binding sites for Ag^+ ion leading to the decolourisation of the chemosensor **BS-2.** This affirmed the interaction between host (herein **BS-2**) and guest analyte (herein Ag^+). The binding constant was calculated to be 2.95 $x10^6$ M^{-1} (**Fig. S11**) from B-H plot using a linear regression equation $1/(A-A_0) = 2.60872 + 7.7045x10^6 \times 1/[Ag^+]$.Absorbance at 270 nm *vs.*concentration of Ag^+ with a good linear regression curve was obtained in the conc. Range of 0-3.4 µM. The LOD was calculated according to above mentioned equation and it was found to be 10.84 µM **(Fig. S12)**.

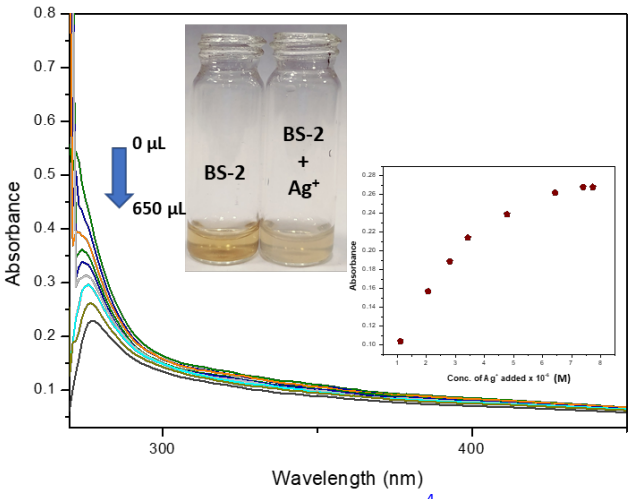

Fig. 6 UV-Vis absorbance change of **BS-2** (10^{-4} M) in DMSO medium with the gradual addition of Ag^+(10^{-4} M) in MeCN:H_2O (9:1; *v/v*) medium at room temperature. Inset: absorbance at 270 nm as a function of the equivalence of Ag^+ ions added.

The selectivity of BS-2 towards other cations in organo-aqueous medium. To evaluate the selectivity of the sensory probe towards Ag^+ ion, we have measured the absorbance response of [BS-2···Ag^+] ion complex in the presence of some competitive interfering metal ions individually (**Fig. S13** & Visual colour change **Fig. 5**). The metal ions mentioned above do not cause any subtle changes on the absorbance of the probe depicting its profound selectivity. Hence, Ag^+ ions can be easily detected by the probe in the co-existence of above metal ions with several-fold of concentrations.

Time-dependent response of BS-1 & BS-2 towards targeted analytes. Quick time-response is one of theessential factors for a chemosensor to detect external stimuli in practical application. The time-dependent absorbance intensity profile of **BS-1** & **BS-2** was carried out in DMSO medium at room temperature in the presence of targeted analytes (*i.e.* for **BS-1** both S^{2-}, Ag^+ and for **BS-2**, only S^{2-}). The plot of absorbance intensities of BS-1 at 315 nm reached the maximum value after 40 sec in the presence of S^{2-} (10^{-4} M, H_2O) whereas for Ag^+ (10^{-4} M, MeCN/H_2O) the responding time is about 1 min (at 410 nm). While for **BS-2** the absorbance intensity at 270 nm, reached a plateau in approximately 1 min for targeted analyte Ag^+ (10^{-4} M, MeCN/H_2O) (**Fig. S14**). The quick response time of BS-1 & BS-2 towards the targeted analytes demonstrated that these sensory receptors might be used for the real-time recognition of S^{2-}, Ag^+ and Ag^+ respectively with naked eye approach.

Cyclic voltammetricstudy of BS-1 with S^{2-} & Ag^+. The electrochemical responses of **BS-1** towards S^{2-} and Ag^+ were examined by cyclic voltammetry (CV) in DMSO medium with $TBAPF_6$ as the supporting electrolyte and the medium was degassed by argon purging.[24] The scan rate of the whole experimental procedure was 0.05 V/Sin a three-electrode configured system. A platinum wire was used as a counter electrode, a saturated calomel electrode (SCE) as the reference electrode and glassy Carbon electrode as a working electrode. All potentials were referenced to the internal standard ferrocenium/ ferrocene (Fc^+/Fc) couple (0.408 eV). All scans were initiated in a positive direction. In the forward scan the chemosensorshowed an intense anodic oxidation potential, E_{pa} at 0.928 V with the current height of -0.022 mA (i_{pa}) whereas in the reverse scan, it showed a cathodic reduction potential, E_{pc}at -0.976 V with the current height of 0.019 mA (i_{pc}). The whole redox event was reversible as $i_{p,c}/i_{pa}$ ~0.9. Initially, on the addition of a small amount of Na_2S (5 µL, 10^{-2}M) there was hardly a change. However, with addition of about 100 µL of S^{2-}solution, some noticeable changes took place in the initial electrochemical responses of **BS-1**. Upon gradual addition of S^{2-}, the position of both redox potentials remained the same; only the anodic potential was shifted to the higher current height from-0.0219 mA to – 0.0295 mA (**Fig. 7**). Upon gradual addition of S^{2-}, there was a steady decrease in the cathodic potential peak with a reduction in current height from 0.0034 mA to 0.0012 mA. Due to the addition of S^{2-}, the chemosensor BS-1 got reduced, facilitating in its oxidation tendency. This easy transfer of electrons was also supported by UV-Vis experimentation, where facile electronic transfer helped in vivid colourimetric responses of host-guest interaction. Likewise, upon addition of a small amount of Ag^+ (5 µL, 10^{-2} M), there was no significant change in the electrochemical responses of the sensory receptor. However, with the gradualaddition of nearly 50 µL of Ag^+ solution, some noticeable change was observed (**Fig. 8**). There was a shifting in the anodic potential from 0.928 V to 1.006 V with an increase of current height of 0.005 mA whereas the cathodic potential shifted to -0.988 V with an increase in current height of 0.004 mA. Moreover, the gradual shifting in the cathodic potential from -0.70 V to -0.74 V with an increase in the current height of 0.0055 mA suggested easier oxidation-reduction pathway.

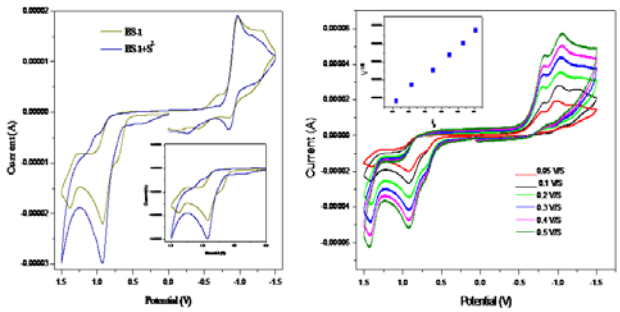

Fig. 7 Electrochemical response of (left) **BS-1** (10^{-3} M) in DMSO with S^{2-} (10^{-2}M) supporting electrolyte, $TBAPF_6$; scan rate, 0.05 V S^{-1} (Right) The effect of redox potential of BS-1 with different scan rate(inset: the reversibility of the redox potential)

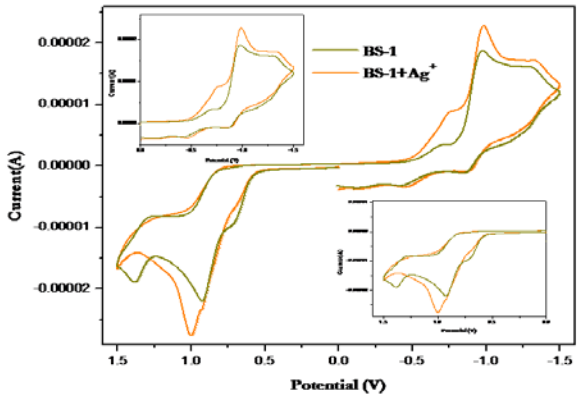

Fig. 8 Electrochemical response of **BS-1** (10^{-3} M) in DMSO with Ag^+ (10^{-2} M) supporting electrolyte, $TBAPF_6$; scan rate, 0.05 V S^{-1}

In both cases, the redox event moves towards quasi-reversible pathway from the reversible process. The extent of the movement towards a quasi-reversible path is higher for S^{2-} than that of Ag^+. **Table 1** & **Table 2** contain the summary of electrochemical responses of **BS-1** after interaction with S^{2-} & Ag^{+}, respectively. In continuation of this, **Fig. 8** shows that the redox event is diffusion controlled.

Table 1. Summary of electrochemical responses of **BS-1** after interaction with S^{2-}

	BS-1	***BS-1 after interaction with S^{2-}***
	Initial	
Oxidation	$E_{p,c}$ = 0.928 V $I_{p,c}$= -0.022 mA	$E_{p,c}$ = 0.928 V $I_{p,c}$= -0.030 mA
Reduction	$E_{p,a}$ = -0.976 V $I_{p,a}$= 0.019 mA	$E_{p,a}$ = -0.976 V $I_{p,a}$ = 0.019 mA

Table 2. Summary of electrochemical responses of **BS-1** after interaction with Ag^+

	BS-1	***BS-1 after interaction with Ag^+***
	Initial	
Reduction	$E_{p,c}$ = -0.976 V $I_{p,c}$= 0.019 mA	$E_{p,c}$ = -0.988 V $I_{p,c}$= 0.023 mA
Oxidation	$E_{p,a}$ = 0.928 V $I_{p,a}$= -0.022 mA	$E_{p,a}$ = 1.006 V $I_{p,a}$ = -0.027 mA

Cyclic voltammetric study of BS-2 with Ag^+. On addition of 50 µL of Ag^+ (10^{-2} M, DMSO) solution to the chemosensor (**BS-2)** solution, generation of a new reduction peak at 0.826 V was observed with a current height of 0.006 mA (**Fig. 9**). Generation of the new cathodic peak was probably due to the dragging of electron density from the molecular scaffold towards Ag^+ showing immense reduction ability of **BS-2**.

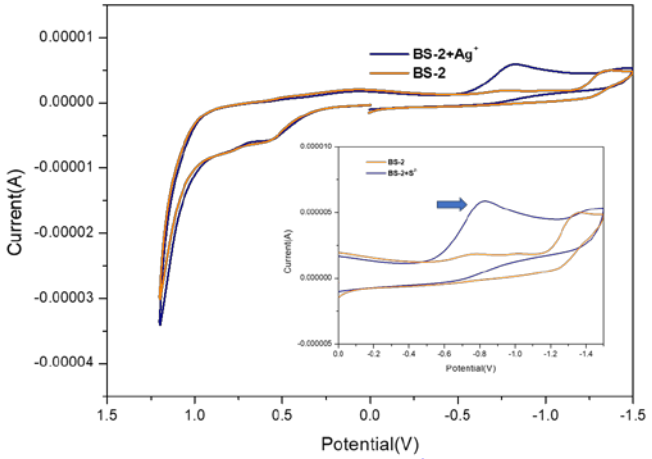

Fig. 9 Electrochemical response of **BS-2** (10^{-3} M) in DMSO with Ag^+ (10^{-2} M) supporting electrolyte, $TBAPF_6$; scan rate, 0.05 V S^{-1}

Infrared spectroscopic evidence of interaction with the targeted analyte. The infrared spectroscopic studies of **BS-1** & **BS-2** were performed in the solid-state using KBr disks. The decrease of the peak intensity at 2056 cm^{-1} and formation of a new broad peak at 3400 cm^{-1} confirms the formation of amine due to the reductionof both terminal and bridging $-N_3$ by S^{2-}(**Fig. S15a**). In continuation, the new vibrational peak at 1584 cm^{-1} also supports the formation of primary amine.[25] Moreover, the reduction [26] of $-N_3$ through the intermediate step [-NH-N=N-SH]$^{\#}$ was also supported by the mass spectrometric analysis(ESI, **Fig. S17**). Apart from this, the appearance of a new peak position at 1390 cm^{-1} was due to the Ag-N bond stretching[27], which inferred the formation of AgN_3 (ESI, **Fig.S15b**). The appearance of a new peak position at 2380 cm^{-1} in case of **BS-2** after addition of Ag^+ supports the formation of labile Ag-N bond[28] (ESI, **Fig. S16**). From the IR spectroscopic analysis, the probable binding centre was foundsupporting the mechanistic point of host-guest interaction.

Theoretical calculations

In order to elucidate the probable mechanistic course of interaction between the host (**BS-1** & **BS-2**) and targeted guest analyte (S^{2-}), Density Functional Theory (DFT), computational calculations, were performed using Turbomole (V 7.0) software. These calculations were done in order to correlate the experimental and theoretical outcomes.

This journal is © The Royal Society of Chemistry 20xx

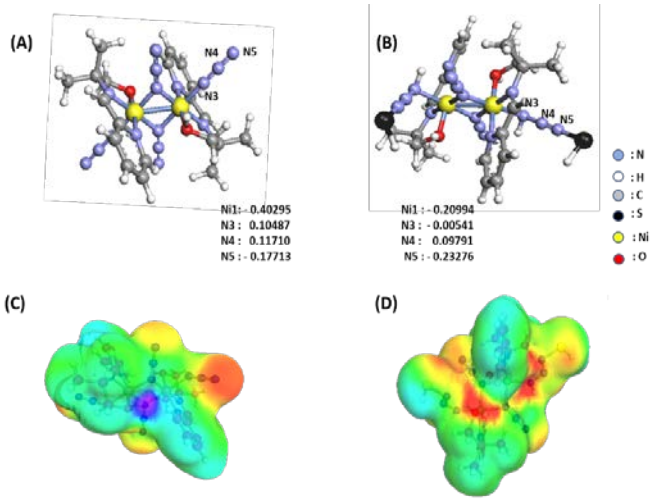

Fig. 10 (A) Energy minimised structure of **BS-1** with its *Loewdin* spin population (B) Energy minimised structure of BS-1 with S^{2-} along with its *Loewdin* spin population (C) & (D) Electrostatic potential surfaces of BS-1& $[BS\text{-}1\cdots S^{2-}]^{\#}$ intermediate respectively viewing electron-deficient (yellow, green, light blue, deep blue) to electron-rich (red) regions.

Initially, the energetically most stable structure (**Fig. 10A**) was taken into consideration for the calculation (at the level of B3LYP hybrid function). After proper geometrical optimisation, the optimised structure was used to study the interaction of binding of the chemoreceptor **BS-1** with the incoming guest S^{2-} which is furthermore strengthened by ESI-MS data. Initially, it was observed that the HOMO was located on the metal centre while the LUMO was located on the aromatic pyridine unit. Interestingly it was found from ***Loewdin*** spin population (**LSP**) that the drifting of electron density took place from the metal centres towards the monodentate azide centres after interaction with S^{2-}, supporting a facile reduction of the azide centres. Moreover, the distance between proton of the aliphatic -OH and the bridged azide centre is 2.58 A^{o},thereby suggesting H-bonding, which further stabilised the $[\mathbf{BS\text{-}1}\text{—}S^{2-}]^{\#}$ intermediate adduct. The total energy of the host-guest intermediate adduct was found to be – 5866.06 KJ mol^{-1} with a HOMO-LUMO gap of 2.79 eV which was lower compared to the $\Delta E_{HOMO\text{-}LUMO}$ of the barechemosensorBS-1(totalenergy = -5067.68 KJ mol^{-1} with a HOMO-LUMO gap of 3.042 eV) (**Fig. 11**). There was no evidence of deprotonation of -OH centres in the experimental as well as in the theoretical outcomes. Moreover, the **LSP** analysis of both the chemosensor and the host: guest adduct was performed using the DFT. It was observed that the monodentate azidecentre (N5) of the **BS-1** (**Fig. 10A & 10B**) after interaction with S^{2-} became electronically rich. As a result, facile reduction of those two monodentateazide centres along with bridging azide centres took place *via* the intermediate {[NH-N=N-SH]$^{\#}$} formation. As an artefact, monomeric Ni-cluster is formed (**Fig. S19**) due to the reduction of bridgingazide to a primary amine, which is also confirmed by FT-IR studies (**Fig. S15**).

Interestingly it was found that after the formation of the monomer unit with two primary amine centres, the HOMO-LUMO energy gap (ΔE=2.206eV) decreases from that of the dimeric cluster (ΔE=3.042 eV) that ultimately supported the mechanistic insights into the sulphide mediated reduction of arylazide. In continuation to this, DFT studies also revealed that $\Delta E_{HOMO\text{-}LUMO}$ for **BS-2** monomeric unit (**Fig. S18**) was 2.275 eV which is higher compared to that of bare chemosensor **BS-2** (1.53 eV) indicating its reluctancetowardsinteraction with S^{2-}. Thus, the logical outcome fully corroborated with the experimental findings.

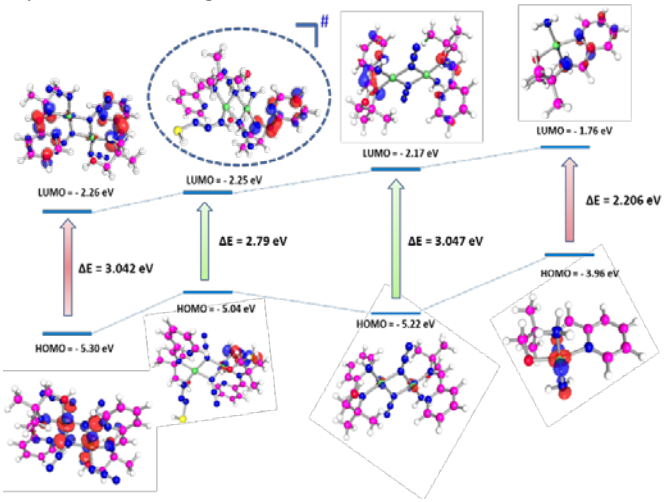

Fig. 11 Optimised structure and HOMO-LUMO band gap of chemosensor**BS-1**,$[\mathbf{BS\text{-}1\text{---}S^{2-}}]^{\#}$adduct and monomer of **BS-1**

Real field application/ Visual colour change on test strips. In order to investigate the practical implementation of the chemosensor **BS-1**, test paper strips were prepared by immersing paper strips (3 x 1 cm^2) into a DMSO solution of **BS-1**(10^{-3}mol/L) followed by air drying for overnight.[29] The test strips were utilised for detection of S^{2-} in the solution phase as well as in gaseous phase *i.e.* detection of H_2S gas was also performed for clear authentication. A distinct colour change was observed from light yellow to brown (**Fig. 12)** when S^{2-}/H_2S came into the vicinity of the paper strips with the help of "***Dip-stick***" approach. Thus detection of this lethal toxic element (S^{2-}/H_2S) can be done on the field instantly using this test strip without the assistance of any costly instrumentation. A comparative literature survey of BS-1 with other S^{2-} & Ag^{+} sensors was also performed (**Table 3**) which expressed the superiority of our developed system.

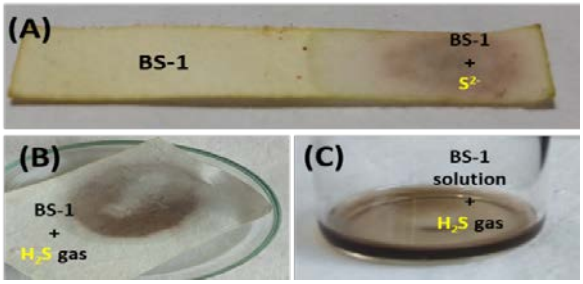

Fig. 12 (A) Test strip coated with **BS-1** sensor upon interaction with S^{2-} (B) Test strip of **BS-1** after interaction with H_2S gas (C) Solution of **BS-1** after interaction with H_2S gas

Conclusions

In brief, we report the synthesis and characterisation of two dinuclear complexes **BS-1** and **BS-2** and their use as molecular sensors towards hazardous entities. Proper tuning of the molecular probe makes the system **BS-1** highly selective for dual sensing of S^{2-} and Ag^{+} while **BS-2** for Ag^{+} only.The sensory probe **BS-1** shows a

detection limit of 0.55 µM for sulphide, which is lower compared to the permissible limit guided by WHO. The experimental findings are fully supported by DFT studies implementing that the H_2S-mediated azide reduction and maybe a crucial step in the refinement of this vital sensing strategy for H_2S. Moreover, the chemosensor **BS-1,** may be exploited towards the fabrication of low-cost teststrips that are very useful in practicaland efficient detection of S^{2-}/H_2S from the aqueous phase.

Acknowledgements

Science& Engineering Research Board (SERB) sponsored project (YSS/2014/000466), Department of Science and Technology (DST)-WTI sponsored project (GAP 214312 *vide* DST/TM/WTI/2k16/277) and CSIR-FTT sponsored project (MLP-223712 *vide* 33/2018/MD-FTT&FTC) are hereby acknowledged for financial assistance. SB gratefully acknowledges Mr. Debanjan Dey and Ms. Riyanka Das for their continuous support and valuable discussions during different studies. Mr. Palash Choudhury, MPML group, CSIR-CMERI is acknowledged for performing TGA.

Conflicts of interest

There are no conflicts of interest to declare

Table 3 Comparative literature survey of BS-1 with other reported S^{2-}/H_2S sensor

Entry	*Sensing ions*	*Matrix*	*Method used*	*LOD*	*Binding constant*	*Reaction time*	*Solid state sensing*	*Remarks*	*References*
1	S^{2-}	H_2O	CV	7.5 µM	-	Instant	No	Tedious sample preparation and not applicable for real field	*30*
2.	S^{2-}	Food	CV	1.0 µM	-	Instant	No	Tedious procedure and usage of costly electrodes	*31*
3.	Thiols &S^{2-}	Effluent water	UV-microplat e assay	2.8 µM	-	15mins	No	Measures in the middle UV region and non-selective	*32*
4.	S^{2-}	Cell-imaging	FL assay	5.0 µM	-	60mins	No	Tedious & multistep probe synthesis & takes long time for detection	*33*
5.	H_2S	serum	FL assay	6.0 µM	-	2mins	No	Tedious procedure for probe synthesis	*34*
6.	H_2S	Cell-imaging	FL assay	2.2 µM	1.83 x 10^{-5}M	Instant	No	Tedious procedure for probe synthesis	*35*
7.	H_2S	Cell-imaging	FL assay	2.6µM	-	60mins	No	Long detection time; not applicable for on-field detection	*36*
8.	i) S^{2-}/H_2S ii) Ag^+	100% aqueous medium for S^{2-} &H_2S; MeCN:H_2O (9:1, *v/v*) medium for Ag^+	Colourim etric	i) 0.55 µM ii) 21.8 µM	i) 3.28x$10^5$$M^{-1}$ ii) 0.55x$10^3$$M^{-1}$	**Instant**	**YES**	**i) Cost-effective, selective, complex based sensory assay ii) Simple synthesis procedure**	***Present work***

CV: cyclic voltammetry; FL: fluorescence

This journal is © The Royal Society of Chemistry 20xx

Journal Name

ARTICLE

References

1 (a) C. B. Tian, Z. H. Li, J.D. Lin, S.T. Wu, S. W. Du and P. Lin, *Eur. J. Inorg. Chem* .2010, 427-437. (b) T. C. Stamatatos, G.S. Papaefstathiou, L.R. MacGillivaray, A. Escuer, R. Vicente, E. Ruiz and S. P. Perlepes, *Inorg.Chem*. 2007, **46**, 8843-8850.

2 S. S. Massoud, F.R. Louka, Y.K. Obaid, R. Vicente, J. Ribas, R.C. Fischer and F. A. Mautner, *Dalton Trans*. 2013, **42**, 3968-3978.

3 A. Escuer, J. Esteban, S. P.Perlepes and T. C. Stamatatos, *Coord. Chem. Rev.* 2014, **275**, 87-129.

4 (a) A. J. Tasiopoulos, A. Vinslava, W. Wernsdorfer, K.A. Abboud and G.Christou, *Angew. Chem., Int. Ed.* 2004, **43**, 2117-2121; (b) S. Osa, Y. Sunatsuki, Y. Yamamoto, M. Nakamura, T. Shimamoto, N. Matsumoto and N. Re, *Inorg. Chem.* 2003, **42**, 5507-5512; (c) J. D. Bois, C. S. Tomooka, J. Hong and M. E. Carreira, *Acc. Chem. Res.* 1997, **30**, 364–372; (d) J. F.Berry,*CommentsInorg. Chem.* 2009, **30**, 28–66. (e) C. T.Saouma, and J. C. Peters, *Coord. Chem. Rev.* 2011, **255**, 920–937. (f) A. Jeremies, S. Gr uschinski, M. Meyer, V. Matulis,O. A. Ivashkevich, K. Kobalz and B. Kersting, *Inorg. Chem.* 2016, **55**, 4, 1843-1853.

5 X. D. Jiang, Y. Su, S. Yue, C. Li, H. Yu, H. Zhang, C. L. Sun and L. J. Xiao, *RSC Adv*. 2015,**5**, 16735-16739.

6 (a) S. K. Kim, D. H. Lee, J. I. Hong and J. Yoon,*Acc. Chem. Res*. 2009, **42**, 23-31; (b) S. Bej, R. Das, N. C. Murmu and P. Banerjee, *Inorg. Chem.* 2020, **59**, 7, 4366–4376; (c) S. Bej, A. Hazra, R. Das, S. K.Saha, M. Corbella and P. Banerjee, *New J. Chem*. 2020, https://doi.org/10.1039/D0NJ02265A

7 (a) R. U. I. Wang, *FASEB*.2002, **16**, 1792–1798.; (b) D. J. Lefer, *Proc. Natl. Acad. Sci. U.S.A.* 2007, **104**, 17907–17908;

8 D. J. Polhemus and D.J. Lefer, *Circulation Research*. 2014, **114**, 730–737.

9 C. Wei, Q. Zhu, W. Liu, W. Chen, Z. Xi and L. Yi, *Org. Biomol. Chem.* 2014, **12**, 479-485.

10 Y. Fujii, T. Funakoshi, K. Unuma, K. Noritake, T. Aki and K. Uemura, *J. Toxicol. Sci.* 2016, **41**, 645–654.

11 R. J. Reiffenstein, W.C. Hulbert and S.H. Roth, *Annu. Rev. Pharmacol. Toxicol*. 1992, **32**, 109–134.

12 T. L. Guidotti, *Int. J.Toxicol*. 2010, **29**, 569–581.

13 S. Bhattacharjee, S. Datta and C. Bhattacharjee, *Desalination*, 2007, **212**, 92–102.

14 R. Foldbjerg, P. Olesen, M. Hougaard, D. A. Dang, H.J. Hoffmann and H. Autrup, *Toxicol. Lett*. 2009, **190**, 156–162.

15 G. Kim, E. Jang, A. M. Page, T. Ding, K. A. Carlson and H. Cao, *RSC Adv.,* 2016, **6**, 95920-95924.

16 G.M. Sheldrick, *Acta Crystallogr. Sect.C Struct. Chem.*2015, **71**, 38.

17 O. V. Dolomanov, L. J. Bourhis, R. J. Gildea, J. A. K. Howard and H. Puschmann, *J. Appl. Crystallogr*. 2009, **42**, 339–341.

18 C. F. Macrae, P. R. Edgington, P. McCabe, E. Pidcock, G. P. Shields, R. Taylor, M. Towler and J. Van De Streek, *J. Appl. Crystallogr*. 2006, **39**, 453–457.

19 T. K. Karmakar, G. Aromí, K. Barindra, A. Ghosh, U. H. Fun, T. Mallah, U. Behrens, X. Solansf and S. K. Chandra, *J. Mater. Chem*. 2006, **16**, 278-285.

20 V. S. Igor, A. Kondinski, K. Y. Monakhov, O. K. Igor and E. V. Grachova, *Inorg. Chem. Front*. 2018, **5**, 160–171.

21 S. Chung, Y. Tseng, C. Chen and S. S. Sun, *Inorg. Chem.* 2011, **50**, 2711–2713.

22 F. Yang, F. Yin, H. Guo, Z. Huang and X. Zhang, *Macrocycl. Chem.* 2010, **67**, 49–54.

23 Y. Fu, X. Zeng, L. Mua, X. Jiang, M. Deng, J. X. Zhang and T. Yamato, *Sensors Actuators B Chem*. 2012, **164**, 69–75.

24 (a) S. Goswami, S. Chakraborty, S. Paul, S. Halder, S. Panja and S. K. Mukhopadhyay, *Org. Biomol. Chem*. 2014, **12**, 3037-3044; (b) M. Carraro, G. Bergamini, M. D. Lauro, G. Modugno, M. Baroncini, P. Ceroni and M. Bonchio,. *Eur. J. Inorg. Chem*. 2016, 3405-3410.

25 L. Sacconi, A. Sabatini and S.P. Gans, *Inorg. Chem*. 1964,**12**, 1772-1774.

26 H. A. Henthorn, and M. D. Pluth, *J. Am. Chem. Soc.* 2015, **137(48)**, 15330-15336.

27 C. Sun, C. Zhang, C. Y. Jiang, Y. Du, Y. Zhao, B. Hu, Z. Zheng and K. O. Christe, *Nat Commun*. 2018, **9**, 1-7.

28 G. Lamming, O. E. Zubir, J.Kolokotroni, C. McGurk, G. Waddell, R. Probert and A.Houlton, *Inorg. Chem*.2016, **55**, 9644-9652.

29 S. Bej, R.Das, H.Hirani, S. Ghosh and P. Banerjee, *New J. Chem*. 2019, **43**, 18098-18109.

30 N. S. Lawrence, L. Jiang, T.G. J. Jones and R.G. Compton, *Anal. Chem*. 2003, **75**, 2054-2059.

31 X. Cao, H. Xu, S. Ding, Y. Ye , X. Ge and L. Yu, *J.Food Chem*. 2015, **194**, 1224-1229.

32 B. Coulomb, F.R. Peillard, E. Palacio, R.D. Rocco and J. L. Boudenne, *J. Microc*. 2017, **132**, 205-210.

33 Y. Qian, J. Karpus, O. Kabil, S. Y. Zhang, H.L. Zhu, R. Banerjee, J. Zhao and C.He, *Nat Commun.* 2011, **2**, 495.

34 J. Wang, H. Yu, Q. Li and S. Shao, *Talanta*. 2015, **144**, 763-768.

35 Z. Hai, Y. Bao, Q. Miao, X. Yi and G. Liang, *Anal. Chem*. 2015, **87**, 2678-2684.

36 K. Wang, H. Peng, N. Ni, C. Dai and B. Wang, *J Fluoresc*.2014, **24**, 1–5.